

# Incommensurate Lattice Distortion in the High Temperature Tetragonal Phase of $\text{La}_{2-x}(\text{Sr},\text{Ba})_x\text{CuO}_4$

Shuichi WAKIMOTO<sup>1</sup> \*, Hiroyuki KIMURA<sup>2</sup>, Masaki FUJITA<sup>3</sup>, Kazuyoshi YAMADA<sup>3</sup>, Yukio NODA<sup>2</sup>, Gen SHIRANE<sup>4</sup>, Genda GU<sup>4</sup>, Hyunkyung KIM<sup>5</sup>, and Robert J. BIRGENEAU<sup>6</sup>

<sup>1</sup>Quantum Beam Science Directorate, Japan Atomic Energy Agency, Tokai, Ibaraki 319-1195, Japan

<sup>2</sup>Institute of Multidisciplinary Research for Advanced Materials, Tohoku University, Sendai 980-8577, Japan

<sup>3</sup>Institute for Material Research, Tohoku University, Katahira, Sendai 980-8577, Japan

<sup>4</sup>Department of Physics, Brookhaven National Laboratory, Upton, New York 11973-5000, USA

<sup>5</sup>Department of Physics, University of Toronto, Toronto, Ontario, Canada M5S 1A7

<sup>6</sup>Department of Physics, University of California, Berkeley, Berkeley, California 94720-7300, USA

We report incommensurate diffuse (ICD) scattering appearing in the high-temperature-tetragonal (HTT) phase of  $\text{La}_{2-x}(\text{Sr},\text{Ba})_x\text{CuO}_4$  with  $0.07 \leq x \leq 0.20$  observed by the neutron diffraction technique. For all compositions, a sharp superlattice peak of the low-temperature-orthorhombic (LTO) structure is replaced by a pair of ICD peaks with the modulation vector parallel to the  $\text{CuO}_6$  octahedral tilting direction, that is, the diagonal Cu-Cu direction of the  $\text{CuO}_2$  plane, above the LTO-HTT transition temperature  $T_s$ . The temperature dependences of the incommensurability  $\delta$  for all samples scale approximately as  $T/T_s$ , while those of the integrated intensity of the ICD peaks scale as  $(T - T_s)^{-1}$ . These observations together with absence of ICD peaks in the non-superconducting  $x = 0.05$  sample evince a universal incommensurate lattice instability of hole-doped 214 cuprates in the superconducting regime.

KEYWORDS:  $\text{La}_{2-x}\text{Sr}_x\text{CuO}_4$ , High- $T_c$  superconductivity, Neutron scattering, Diffuse scattering

## 1. Introduction

After the discovery of the high-transition-temperature (high- $T_c$ ) superconductivity, extensive efforts have been made in this research field for almost two decades. Although the mechanism of the Cooper pair formation in the high- $T_c$  systems still requires more clues to be properly understood, it is widely expected that the incommensurate magnetic state is intimately related to the superconductivity. In fact, neutron scattering experiments for the hole-doped superconductor  $\text{La}_{2-x}\text{Sr}_x\text{CuO}_4$  have revealed incommensurate magnetic fluctuations<sup>1,2</sup> which exists up to the critical hole concentration where the superconductivity disappears.<sup>3</sup> Such incommensurate magnetic fluctuations have been frequently ascribed to a dynamic microscopic phase separation into hole-free magnetic regions divided by hole-rich stripes,<sup>4-8</sup> which may suggest that the high- $T_c$  systems are intrinsically unstable to stripe-like formation on fundamental lattices.

By x-ray scattering techniques, incommensurate diffuse (ICD) peaks have been observed with modulation vectors along the orthorhombic  $a$ - and  $b$ -axes, that is, along the diagonal Cu-Cu direction of the  $\text{CuO}_2$  plane, in the low-temperature-orthorhombic (LTO) phase of  $\text{La}_{2-x}\text{Sr}_x\text{CuO}_4$  and  $\text{La}_{2-x}\text{Sr}_x\text{NiO}_4$ .<sup>9,10</sup> Later, a coexistence of two types of  $\text{CuO}_6$  octahedral tilt, one of the LTO type and the other of the low-temperature-tetragonal (LTT) type, have been reported by x-ray absorption fine structure (EXAFS) and x-ray absorption near edge structure (XANES) measurements although the average crystal structure is LTO.<sup>11,12</sup> From these results it has been hypothesized that a local LTT structure exists in a stripe form in the LTO phase.

Similar to this, it has been reported that an LTO type octahedral tilt also remains locally in the high-temperature-tetragonal (HTT) phase in  $\text{La}_{2-x}\text{Sr}_x\text{CuO}_4$  by EXAFS,<sup>13</sup> nuclear magnetic resonance (NMR),<sup>14</sup> and neutron diffraction.<sup>15,16</sup> By neutron measurements, Kimura *et al.*<sup>16</sup> have observed a local LTO-type distortion in the HTT phase of  $\text{La}_{2-x}\text{Sr}_x\text{CuO}_4$  with  $x = 0.12$  and  $0.18$ . The evidence for this is incommensurate diffuse peaks at  $((n \pm \delta)/2, (n \pm \delta)/2, m)$  ( $n$ :odd,  $m$ :even) as shown by the open circles in Fig. 1(a). Note that in this expression the incommensurability  $\delta$  is equivalent to the distance between the ICD peak and the LTO superlattice position expressed in orthorhombic reciprocal lattice units (r.l.u.). This modulation direction corresponds to, again, the diagonal Cu-Cu direction. Moreover, the incommensurability  $\delta$  for the two concentrations scales approximately as the normalized temperature  $T/T_s$  where  $T_s$  is the LTO-HTT transition temperature. Recently, it has been reported that no such incommensurate diffuse feature can be detectable in the non-superconducting  $x = 0.05$  sample,<sup>17</sup> suggesting a correlation between the incommensurate structural instability and the superconductivity.

In the present paper, we report the observation of incommensurate diffuse scattering in the HTT phase studied by neutron diffraction using single crystals of  $\text{La}_{2-x}(\text{Sr},\text{Ba})_x\text{CuO}_4$  with  $x = 0.07, 0.125, 0.15$  and  $0.20$ . These samples cover a wide concentration range from the underdoped to slightly overdoped regions. The intent of these measurements is to understand the relation between the structural instability and the superconductivity.

\*E-mail address: wakimoto.shuichi@jaea.go.jp

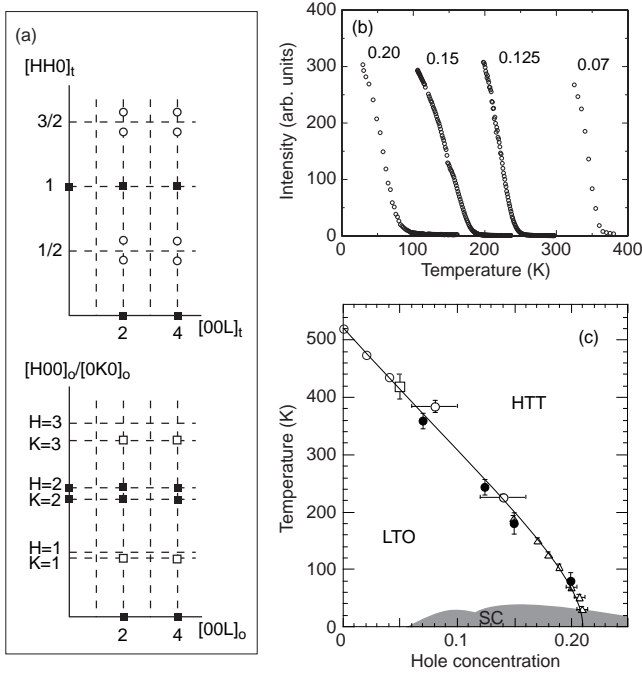


Fig. 1. (a) Neutron scattering peak geometries for  $T > T_s$  (top) and  $T < T_s$  (bottom). The closed square, open squares, and open circles represent the nuclear Bragg peaks, superlattice peaks in the LTO phase, and the incommensurate diffuse peaks, respectively. (b) Temperature dependence of the superlattice peak intensity measured at the (014) position in the LTO notation. (c) Hole concentration dependence of the LTO-HTT transition temperature  $T_s$ . The open symbols are data referred from refs 17, 20–23, while the closed symbols represent  $T_s$  of the present samples which are derived by a linear extrapolation of the temperature dependence of superlattice peak intensity to zero.

## 2. Experimental Details

Single crystals of  $\text{La}_{2-x}\text{Sr}_x\text{CuO}_4$  (LSCO) with  $x = 0.07, 0.15$ , and  $0.20$  and  $\text{La}_{2-x}\text{Ba}_x\text{CuO}_4$  (LBCO) with  $x = 0.125$  were grown by the traveling-solvent floating-zone method.<sup>18,19</sup> All crystals underwent post-growth anneal in an oxygen atmosphere to remove any oxygen deficiencies. The typical sample size was 7 mm in diameter and 30 mm in length. Neutron scattering experiments were performed at the TOPAN thermal neutron triple-axis spectrometer and the LTAS cold neutron triple axis spectrometer at the Japan Atomic Energy Agency in Tokai, Japan.

ICD peaks of LSCO with  $x = 0.15$  and LBCO with  $x = 0.125$  were measured mainly at the  $(3/2, 3/2, 2)$  position using TOPAN with a collimation sequence of B-60'-60'-B and an incident neutron energy  $E_i = 13.5$  meV ( $\lambda = 2.46$  Å), and those of LSCO with  $x = 0.07$  and  $0.20$  were studied mainly at  $(1/2, 1/2, 4)$  using LTAS with G-80'-80'-B and  $E_i = 5$  meV ( $\lambda = 4.05$  Å). Pyrolytic graphite and Be filters were utilized for the TOPAN and the LTAS spectrometers, respectively, to remove neutrons with higher harmonic wave length ( $\lambda/2, \lambda/3$ , etc.).

All samples show a structural transition from the HTT to the LTO structures. Figure 1(a) depicts the peak geometries in the reciprocal lattice above (top) and below (bottom) the transition temperature  $T_s$ . In the LTO

phase ( $T < T_s$ ), superlattice peaks appear at positions such as (014) and (032) shown by the open squares. Note that in the LTO phase the orthorhombic  $a$ - and  $b$ -axes are superposed due to the twinned structure. As temperature increases above  $T_s$ , the superlattice peak is replaced by weak incommensurate diffuse peaks as shown by the open circles in Fig. 1(a) (Top). Figure 1(b) shows the temperature dependence of the superlattice peak intensity for all samples measured at the (014) position.  $T_s$  is determined to be 359 K, 241 K, 180 K, and 80 K for  $x = 0.07, 0.125, 0.15$ , and  $0.20$ , respectively, by a linear extrapolation of the superlattice peak intensity to zero. Those values are summarized in Fig. 1(c) together with those for different concentrations reported previously.<sup>17,20–23</sup> It is shown that the present crystals have Sr contents that vary systematically and are consistent with the nominal compositions.

In the present paper, we utilize tetragonal notation to express the  $\mathbf{Q}$  positions of the incommensurate diffuse peaks in the HTT phase. The tetragonal notation gives  $a = 3.8$  Å and  $c = 13.1$  Å, corresponding to reciprocal lattice units  $a^* = 1.65$  Å<sup>-1</sup> and  $c^* = 0.47$  Å<sup>-1</sup>, while the orthorhombic reciprocal lattice unit is to  $a^*/\sqrt{2} = 1.17$  Å<sup>-1</sup>.

## 3. Results

We have observed incommensurate diffuse peaks in the HTT phase for all of the present crystals. Figure 2(a) is a representative contour plot of the ICD peaks of LBCO  $x = 0.125$  measured at 315 K around the  $(1/2, 1/2, 4)$  position in the  $HHL$  scattering plane. As the ICD peaks are observed clearly in the LBCO sample, the ICD feature in the HTT phase appears to be common in the hole-doped 214 compounds. We have scanned along the  $[H-H0]$  direction at the ICD peak position by changing the tilt angle of the sample. This scan indicates that the ICD peaks are located primarily on the  $HHL$  plane, that is, the modulation direction is the  $[HH0]$  direction which corresponds to the diagonal Cu-Cu direction on the  $\text{CuO}_2$  plane.

To study the  $\mathbf{Q}$ -dependence, we have measured the ICD peaks in different zones. Figures 2(b) and 2(c) show peak profiles at 450 K along the  $[HH0]$  direction at the  $(3/2, 3/2, 2)$  and  $(1/2, 1/2, 4)$  positions, respectively. We note that there is an intensity imbalance between the ICD peaks, which increases as the temperature increases. It is also notable that the intensity imbalance alters between the  $(3/2, 3/2, 2)$  and  $(1/2, 1/2, 4)$  zones, that is, the ICD peak at smaller  $H$  is higher in the former zone whereas that at larger  $H$  is higher in the latter. Those features are commonly observed in all of the present samples.

The profiles in Figs. 2(b) and 2(c) have been fitted to a resolution-convoluted two-dimensional (2D) Lorentzian function

$$S(\mathbf{Q}) = |F(\mathbf{Q})|^2 \left[ \frac{1}{1 + (\mathbf{q} - \mathbf{q}_\delta)^2 \xi^2} + \frac{\alpha}{1 + (\mathbf{q} - \mathbf{q}_{-\delta})^2 \xi^2} \right], \quad (1)$$

where  $F(\mathbf{Q})$  is the structure factor,  $\mathbf{q}_{\pm\delta}$  is the ICD peak positions,  $\xi$  is the correlation length, and  $\alpha$  is a factor to compensate for the intensity imbalance. The spectrum

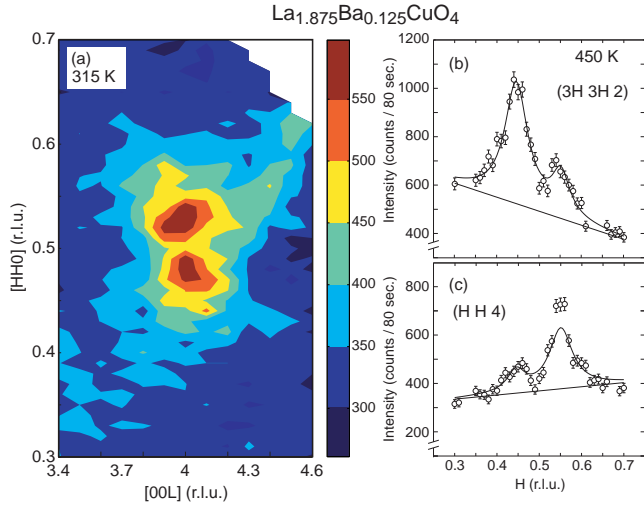


Fig. 2. (a) Contour plot of the incommensurate diffuse peaks around  $(1/2, 1/2, 4)$  of  $\text{La}_{1.875}\text{Ba}_{0.125}\text{CuO}_4$  measured at 315 K. (b) and (c) show incommensurate peak profiles around  $(3/2, 3/2, 2)$  and  $(1/2, 1/2, 4)$ , respectively, measured at 450 K along the  $[HH0]$  direction. The solid lines in (b) and (c) are the results of fits to a resolution-convoluted 2D Lorentzian function and adjusted background levels.

distribution along the energy transfer ( $\omega$ ) direction is assumed to be well-concentrated at  $\omega = 0$ , since, as shown later, the ICD signal is consistently observed by using the cold neutrons which give finer energy resolution. The fits so-obtained are shown by the solid curves in Figs. 2(b) and 2(c), where the background levels have also been adjusted.

Figures 2(b) and 2(c) show larger diffuse intensity in the  $(3/2, 3/2, 2)$  zone. From the fitting parameters, we find the ratio of  $|F(\mathbf{Q})|^2(1 + \alpha)$ , which corresponds to the summation of the peak intensities, between  $(3/2, 3/2, 2)$  and  $(1/2, 1/2, 4)$  to be 1.8. This value is consistent with the ratio of  $|F(\mathbf{Q})|^2$  of the LTO superlattice peaks at  $(032)$  and  $(014)$  in the orthorhombic notation,  $|F(032)|^2/|F(014)|^2 = 1.96$ , suggesting that the ICD peaks originate from the atomic displacements corresponding to the LTO type octahedral tilts.

We have studied the temperature dependence of the ICD peaks. Figure 3(a) shows the temperature dependence of the ICD peaks of the LSCO  $x = 0.20$  sample around  $(1/2, 1/2, 4)$  measured along the  $[HH0]$  direction. Note that these profiles are taken by using cold neutrons with  $E_i = 5$  meV, while the data in Fig. 2 are taken by using thermal neutrons with  $E_i = 13.5$  meV. We have observed qualitatively similar behavior of the ICD peaks for all of the samples in regardless of the neutron energy. We show the data of LSCO  $x = 0.20$  representatively to report the temperature dependences of physical quantities since the  $x = 0.20$  sample has the lowest  $T_s$  among the samples; hence, we are able to study the ICD peaks up to reasonably high temperatures with respect to  $T_s$ . Figure 3(a) clearly demonstrates that a commensurate peak near the transition temperature  $T_s$  is replaced by incommensurate diffuse peaks at higher temperatures with an incommensurability that increases with increasing tem-

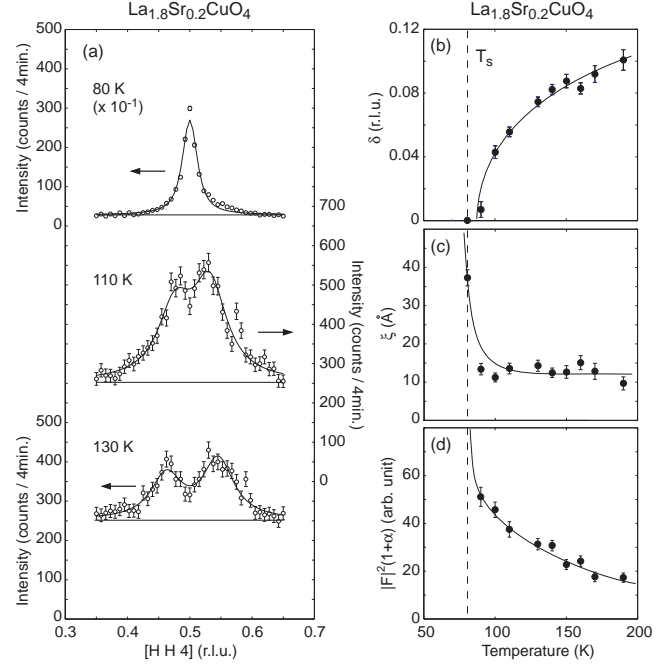


Fig. 3. (a) Temperature variation of the diffuse peak profile measured at  $(1/2, 1/2, 4)$  for  $\text{La}_{1.8}\text{Sr}_{0.2}\text{CuO}_4$ . The solid lines are fits to a resolution-convoluted 2D Lorentzian function and adjusted background levels. (b), (c), and (d) show temperature dependences of the incommensurability  $\delta$ , the correlation length  $\xi$ , and  $|F|^2(1 + \alpha)$ , respectively, derived from the fitting results. Solid lines are guides to the eye.

perature.

To draw more details, we analyze the data by fitting to the resolution-convoluted 2D Lorentzian function described in eq. (1). The results of fits are shown by the solid lines in Fig. 3(a) and the parameters are summarized in Figs. 3(b), 3(c) and 3(d). The incommensurability  $\delta$  decreases as temperature decreases and reaches zero near  $T_s$ , while the correlation length  $\xi$  stays constant in the incommensurate region and diverges near  $T_s$ . The quantity  $|F|^2(1 + \alpha)$  which corresponds to the summation of the peak intensities increases gradually as temperature decreases and shows a rapid increase near  $T_s$ . These behaviors of the fitting parameters are commonly observed for all samples. Interestingly, the deconvolution analyses exhibit a constant correlation length of  $\sim 15$  Å above  $T_s$  for all samples. We show more details of the incommensurability and the integrated intensity later. Also, a possible microscopic picture of these phenomena is discussed in the next section.

Kimura *et al.*<sup>16</sup> have reported that the temperature dependences of  $\delta$  for the LSCO  $x = 0.12$  and  $0.18$  samples fall onto an identical line by utilizing a normalized temperature  $T/T_s$ . We have tested if this applies to a wider concentration range. Figure 4(a) shows the temperature dependence of the incommensurability  $\delta$  for all samples. It is found that, particularly by comparison between the data of  $x = 0.20$  and  $0.07$ , the gradient of the increase of  $\delta$  is apparently smaller for samples with higher  $T_s$ . Such behavior is consistent with the scaling feature of  $\delta$  by  $T/T_s$ . In fact,  $\delta$  approximately falls onto a universal curve as a

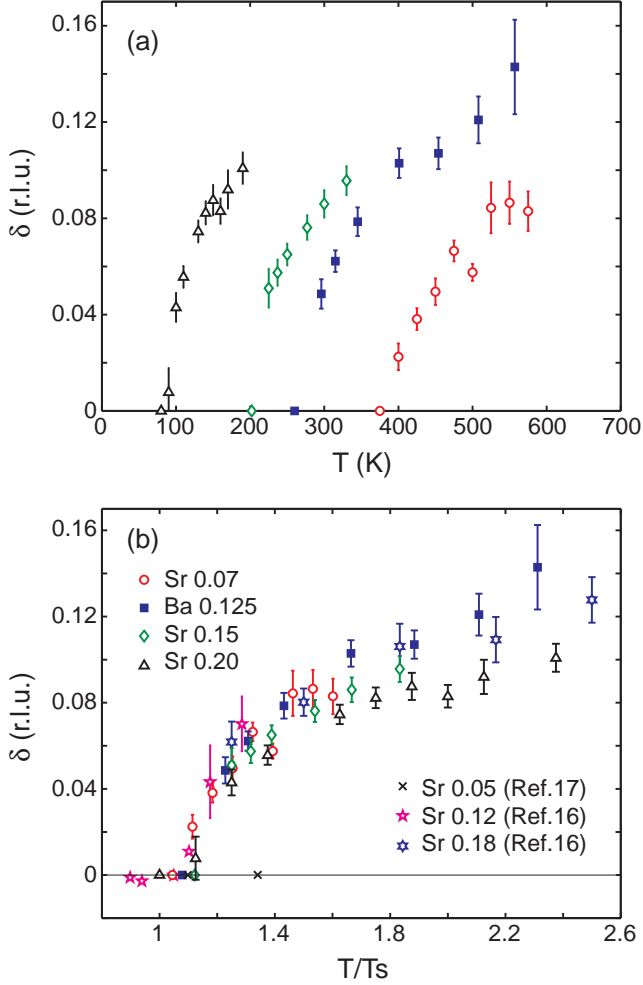


Fig. 4. (Color online) Incommensurability  $\delta$  for all of the present samples as a function of (a) temperature and (b) normalized temperature  $T/T_s$ . In (b) data of Sr  $x = 0.12$  and  $0.18$  from ref. 16, and of  $x = 0.05$  from ref. 17 are also shown.

function of  $T/T_s$  as shown in Fig. 4(b). Although, at high  $T/T_s (> 1.8)$ , there are discrepancies between the data of  $x = 0.125$  and  $0.20$ ,  $\delta(T/T_s)$  agrees for the temperature range of  $1 \leq T/T_s \leq 1.5$ . Since the universality holds for data measured by both thermal and cold neutrons, i.e. different energy resolutions, we conclude that the ICD feature is static and intrinsic rather than being caused by a spurious process, such as detecting phonons at the edge of resolution ellipsoid.

As reviewed in the introduction, the ICD peaks were absent for the LSCO  $x = 0.05$  sample.<sup>17</sup> For this sample it has been confirmed that there is a weak commensurate diffuse peak up to 550 K ( $T/T_s \sim 1.34$ ). Data for  $x = 0.05$  are plotted by crosses in Fig. 4(b). Remarkably, the diffuse peak of the non-superconducting  $x = 0.05$  sample stays commensurate at  $T/T_s = 1.34$  whereas the present superconducting samples show an incommensurability of 0.06 r.l.u. at the reduced temperature. This demonstrates that the ICD feature is characteristic to the superconducting samples.

To test if there is any unusual enhancement of the ICD peaks at a certain hole concentration, we compared integrated intensities, which have been derived by fitting

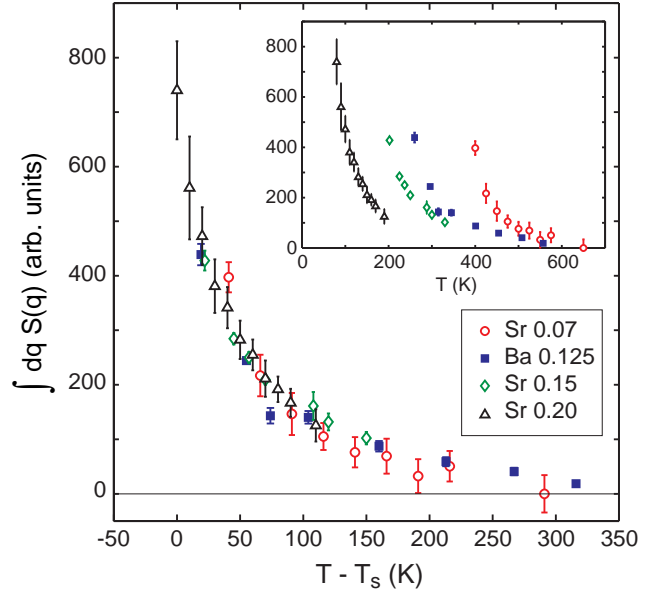


Fig. 5. (Color online) Normalized integrated intensity  $\int dq S(q)$  for all of the present samples as a function of  $T - T_s$ . The inset shows same quantities as a function of temperature.

the profiles to a simple Gaussian function and integrating the intensity along the [HH0] scan direction. The derived integrated intensities have been normalized to sample volume, resolution volume, and structure factors. Sample volume and resolution volume are determined by acoustic phonon measurements around  $(1, 1, 0)$ , while the structure factor ratio of 1.8 between  $(3/2, 3/2, 2)$  and  $(1/4, 1/4, 4)$  is adopted from the data of  $x = 0.125$  in Figs. 2(b) and 2(c). Note that, although the normalization to the resolution volume may have some uncertainty, each comparison between the samples of  $x = 0.07$  and  $0.20$ , and between the samples of  $x = 0.125$  and  $0.15$  is robust since each pair has been measured under an identical spectrometer configuration, respectively. The normalized integrated intensities,  $\int dq S(q)$ , so-obtained are summarized in Fig. 5 as a function of  $T - T_s$ . The inset shows the same quantities as a function of temperature. The excellent agreement of  $\int dq S(q)$  for all samples indicates that there is no particular enhancement of the ICD peak at a certain hole concentration.

#### 4. Discussion

We have shown that the hole-doped 214 cuprates have universal incommensurate diffuse scattering in the HTT phase. From the comparison to the non-superconducting  $x = 0.05$  sample in Fig. 4, it is very likely that the ICD feature is unique to the superconducting samples. It is also important to study superconducting samples without structural transition, such as overdoped samples. Our preliminary measurements of the superconducting  $x = 0.25$  sample at 12 K appear to exhibit very weak ICD peaks with  $\delta \sim 0.1$  r.l.u. Thus, we believe that there is a universal local lattice instability towards the incommensurate octahedral tilt distortion in the superconducting samples. If the system has a structural transition, the incommensurability is suppressed following the universal



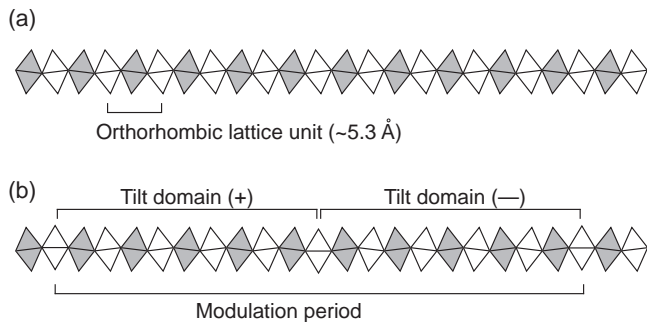


Fig. 6. (a) CuO<sub>6</sub> octahedral tilts in the LTO phase viewed from the orthorhombic  $a$ -axis. (b) An example of modulated tilting pattern which causes incommensurate peaks. Antiphased tilting domains are recognized as domain (+) and (-). Depicted modulation period is 10 orthorhombic lattice units giving the incommensurability of 0.10 r.l.u.

curve in Fig. 4 at the temperature range of  $T/T_s \leq 1.5$ .

Bianconi *et al.*<sup>11</sup> hypothesized that a LTT-type local lattice distortion exists in a stripe form in the LTO background to explain the incommensurate diffuse scattering in the LTO phase. A similar explanation appears to be relevant to the present observations of the ICD peaks in the HTT phase; that is, LTO-type octahedral tilts remain locally in the HTT phase with a one-dimensional modulation.

As shown in Fig. 1(a), the observed ICD peaks split in the  $HHL$  scattering plane. This means that the modulation vector is parallel to the LTO-type octahedral tilt-direction. Note that if the modulation vector is perpendicular to the tilting direction, the ICD peaks should split from the  $(3/2, 3/2, 2)$  and  $(1/2, 1/2, 4)$  positions along the perpendicular direction to the scattering plane.

An example of the modulated octahedral tilting pattern that gives the observed incommensurate geometry is depicted in Fig. 6(b), while Fig. 6(a) shows uniform octahedral tilts, that give commensurate superlattice peak, viewed from the direction perpendicular to the tilting direction. The modulation period depicted in Fig. 6(b) is 10 orthorhombic lattice units, consisting of 5-lattice each of antiphase tilting domains, indicated by domains (+) and (-), which results in an incommensurability of 0.1 r.l.u. Those domains may form stripes running perpendicular to the tilting direction. Alternatively, a tilting pattern with a varying tilt-angle instead of the stacking of antiphase tilting domains gives qualitatively the same incommensurate geometry. The neutron scattering technique is, however, unable to distinguish between these patterns. If we assume a uniform tilt-angle of the octahedra in a single tilting domain as depicted in Fig. 6(b), the modulation period observed to be more than 50 Å is much longer than the observed correlation length of  $\sim 15$  Å. Thus it might be natural to consider a varying tilt-angle with modulation. Either model, however, does not affect the present discussions.

From the temperature dependence of the parameters in Fig. 3, a possible microscopic picture can be suggested as follows. At very high temperature  $T/T_s \sim 2.5$ , local lattice distortions of the LTO structure start to appear in

a one-dimensional form aligned parallel to the diagonal Cu-Cu direction. At this point, each LTO stripe is thin and close to each other resulting in a small modulation period and large incommensurability. As the temperature decreases, the LTO stripes grow thicker by merging with each other, resulting in larger modulation period and smaller incommensurability. In this growing process, the striped phase has a constant correlation length  $\sim 15$  Å. Either by growing the volume of the striped phase or by enlarging the octahedral tilt-angle, the quantity of  $|F|^2(1 + \alpha)$  and integrated intensity increases. Finally, the modulated phase evolves into a uniform tilt phase, and the correlation length diverges at  $T_s$ .

We note that, with decreasing temperature, the diffuse scattering becomes commensurate at  $T/T_s \sim 1.15$  whereas the system shows the structural phase transition at the lower temperature  $T/T_s = 1$ . The difference  $T/T_s = 0.15$  corresponds to 10 to 30 K in actual temperature scale depending on  $T_s$ . We infer that there is a crossover from the incommensurate to the commensurate states at  $T/T_s \sim 1.15$  where the size of the tilt domain, i.e., the coherence length of the in-phase tilting, far exceeds the correlation length scale which is nearly constant at  $\sim 15$  Å. Then the structural phase transition takes place at lower temperature where the correlation length diverges.

Although the model of local LTO distortion in a one-dimensional (stripe) form explains qualitatively the present observations, a few features still need to be clarified. As mentioned in the previous section, a simple structure factor calculation can reproduce the ratio of the integrated intensity between  $(3/2, 3/2, 2)$  and  $(1/2, 1/2, 4)$ . The change of imbalance, however, of the ICD peaks between these positions cannot be explained by the structure factor calculations based on the tilting pattern depicted in Fig. 6(b). From the structure factor definition, the imbalance of the ICD peaks, i.e. the dependence of ICD intensity along the  $[HH0]$  direction, should originate from atomic displacements parallel to the tilting directions. In the coordinates of the CuO<sub>6</sub> octahedral tilts, only apical oxygen atoms displace towards the tilting direction. However, the structure factors of striped LTO-type tilts predicts larger ICD intensities at the higher  $H$  position at both  $(3/2, 3/2, 2)$  and  $(1/2, 1/2, 4)$ . Thus, the unexpected change of imbalance at different zones may imply additional displacements of in-plane oxygen atoms along the tilt direction. In this aspect, it is interesting to note possible correlations between the present ICD feature and the anomalous softening of Cu-O bond stretching mode observed by x-ray measurements.<sup>24</sup> Both phenomena are observed in the superconducting regime, and, moreover, the latter feature may cause anomalous displacements of in-plane atoms. More detailed measurements of the local structure are necessary to draw firm conclusions.

It is still an open question whether such incommensurate lattice distortion correlates directly with the formation of the magnetic incommensurate state at much lower temperatures. Kimura *et al.*<sup>16</sup> have reported that the incommensurability of the ICD peaks saturates at about 0.12 r.l.u. at high temperatures which value is close

to the incommensurability of the magnetic state at low temperatures and thus they claimed an incipient lattice distortion starting at high temperatures. Present result of the incommensurability as a function of  $T/T_s$  for a wide concentration range suggests a gradual increase of  $\delta$  rather than saturation at high temperatures. Moreover, the incommensurate modulation direction of the lattice distortion in the HTT phase of the present results and in the LTO phase observed by the x-ray measurements is consistently parallel to the diagonal Cu-Cu direction which is  $45^\circ$  away from the magnetic incommensurate modulation direction. Therefore it is unlikely that the lattice distortion is the direct origin of the charge and spin stripes.

Although not being the direct origin of the putative charge and magnetic stripes, the local lattice distortion can affect the charge stripes as a pinning potential. In the hole-doped 214 cuprates, magnetic stripe order is achieved in both a LTO phase and a LTT phase. Neutron scattering measurements report that the magnetic incommensurate peaks in the reciprocal space form rectangles elongated along the orthorhombic  $b$ -axis in the LTO phase,<sup>25,26</sup> while complete squares are observed in the LTT phase.<sup>27,28</sup> Since the LTT-type distortion pins the charge stripes more efficiently, entire stripes will be pinned in the uniform LTT phase, giving a square geometry of the IC peaks. On the other hand, by assuming a LTT distortion in a stripe form running along the orthorhombic  $b$ -axis in an LTO background, the vertical charge stripes are pinned only at the intersections with the diagonal LTT stripes. In this case, the charge stripes may order in a smectic form, which results in a rectangular geometry of the IC magnetic peaks. Thus, the hypothesis of the lattice distortion in a stripe form appears to be consistent with the observations of the magnetic stripes.

In summary, we have studied incommensurate diffuse peaks appearing around the LTO superlattice positions with modulation vector along the diagonal Cu-Cu direction in the HTT phase of the hole-doped 214 cuprates. By comparison of the structure factors at different zones, we conclude that the ICD peaks originate from LTO type displacements, which suggests that a LTO type local lattice distortion remains in a one-dimensionally modulated form in the HTT phase.

### Acknowledgment

The authors thank T. Goto, A. Oosawa, K. Kakurai, S. Laroche, C.-H. Lee, M. Matsuda, and N. Metoki for invaluable discussions. The present work was supported by the US-Japan Cooperative Research Program on Neutron Scattering. Work at the University of Toronto is part of the Canadian Institute of Advanced Research and supported by the Natural Science and Engineering Research Council of Canada. Research at Tohoku University is supported by a Grant-In-Aid for Young Scientists B (13740216 and 15740194) and a Grant-in-Aid from the Japanese Ministry of Education, Culture, Sports, Science and Technology, while work at BNL is supported by the U. S. DOE under contact No. DE-AC02-98CH10886. The work at Lawrence Berkeley Laboratory is supported by

the Office of Basic Energy Sciences, U.S. Department of Energy under contract number : DE-AC03-76SF00098.

- 1) S.-W. Cheong, G. Aeppli, T. E. Mason, H. Mook, S. M. Hayden, P. C. Canfield, Z. Fisk, K. N. Clausen and J. L. Martinez: Phys. Rev. Lett. **67** (1991) 1791.
- 2) K. Yamada, C. H. Lee, K. Kurahashi, S. Wakimoto, S. Ueki, H. Kimura, Y. Endoh, S. Hosoya, G. Shirane, R. J. Birgeneau, M. Greven, M. A. Kastner and Y. J. Kim: Phys. Rev. B **57** (1998) 6165.
- 3) S. Wakimoto, H. Zhang, K. Yamada, I. Swainson, H. Kim and R. J. Birgeneau: Phys. Rev. Lett. **92** (2004) 217004.
- 4) J. M. Tranquada, B. J. Sternlieb, J. D. Axe, Y. Nakamura and S. Uchida: Nature **375** (1995) 561.
- 5) K. Machida: Physica C **158** (1989) 192.
- 6) H. J. Schulz: J. Phys. France **50** (1989) 2833.
- 7) J. Zaanen and O. Gunnarsson: Phys. Rev. B **40** (1989) 7391.
- 8) V. J. Emery, S. A. Kivelson and O. Zachar: Phys. Rev. B **56** (1997) 6120.
- 9) E. D. Isaacs, G. Aeppli, P. Zschack, S.-W. Cheong, H. Williams and D. J. Buttrey: Phys. Rev. Lett. **72** (1994) 3421.
- 10) W. Dmowski, R. J. McQueeney, T. Egami, Y. P. Feng, S. K. Sinha, T. Hinatsu and S. Uchida: Phys. Rev. B **52** (1995) 6829.
- 11) A. Bianconi, N. L. Saini, A. Lanzara, M. Missori, T. Rossetti, H. Oyanagi, K. Oda and T. Ito: Phys. Rev. Lett. **76** (1996) 3412.
- 12) N. L. Saini, A. Lanzara, H. Oyanagi, H. Yamaguchi, K. Oda, T. Ito and A. Bianconi: Phys. Rev. B **55** (1997) 12759.
- 13) D. Haskel, E. A. Stern, D. G. Hinks, A. W. Mitchell, J. D. Jorgensen and J. I. Budnick: Phys. Rev. Lett. **76** (1996) 439.
- 14) T. Goto, M. Ueda, H. Sumikawa, T. Suzuki, M. Fujita, K. Yamada, T. Adachi and Y. Koike: Proceeding of the 24th International Conference on Low Temperature Physics.
- 15) M. Braden, M. Meven, W. Reichardt, L. Pintschovius, M. T. Fernandez-Diaz, G. Heger, F. Nakamura and T. Fujita: Phys. Rev. B **63** (2001) 140510.
- 16) H. Kimura, K. Hirota, C.-H. Lee, K. Yamada and G. Shirane: J. Phys. Soc. Jpn. **69** (2000) 851.
- 17) S. Wakimoto, S.-H. Lee, P. M. Gehring, R. J. Birgeneau and G. Shirane: J. Phys. Soc. Jpn. **73** (2004) 3413.
- 18) S. Hosoya, C. H. Lee, S. Wakimoto, K. Yamada and Y. Endoh: Physica C **235-240** (1994) 547.
- 19) C. H. Lee, N. Kaneko, S. Hosoya, K. Kurahashi, S. Wakimoto, K. Yamada and Y. Endoh: Supercond. Sci. Technol. **11** (1998) 891.
- 20) B. Keimer, N. Belk, R. J. Birgeneau, A. Cassanho, C. Y. Chen, M. Greven, M. A. Kastner, A. Aharony, Y. Endoh, R. W. Erwin and G. Shirane: Phys. Rev. B **46** (1992) 14034.
- 21) H. Takagi, R. J. Cava, M. Marezio, B. Batlogg, J. J. Krajewski, W. F. Peck, Jr., P. Bordet and D. E. Cox: Phys. Rev. Lett. **68** (1992) 3777.
- 22) T. Suzuki, T. Goto, K. Chiba, T. Shinoda, T. Fukase, H. Kimura, K. Yamada, M. Ohashi and Y. Yamaguchi: Phys. Rev. B **57** (1998) R3229.
- 23) H. Kimura, K. Hirota, H. Matsushita, K. Yamada, Y. Endoh, S. -H. Lee, C. F. Majkrzak, R. Erwin, G. Shirane, M. Greven, Y. S. Lee, M. A. Kastner and R. J. Birgeneau: Phys. Rev. B **59** (1999) 6517.
- 24) T. Fukuda, J. Mizuki, K. Ikeuchi, K. Yamada, A. Q. R. Baron and S. Tsutsui: Phys. Rev. B **71** (2005) 060501(R).
- 25) Y. S. Lee, R. J. Birgeneau, M. A. Kastner, Y. Endoh, S. Wakimoto, K. Yamada, R. W. Erwin, S.-H. Lee and G. Shirane: Phys. Rev. B **60** (1999) 3643.
- 26) H. Kimura, H. Matsushita, K. Hirota, Y. Endoh, K. Yamada, G. Shirane, Y. S. Lee, M. A. Kastner and R. J. Birgeneau: Phys. Rev. B **61** (2000) 14366.
- 27) J. M. Tranquada, J. D. Axe, N. Ichikawa, Y. Nakamura, S. Uchida and B. Nachumi: Phys. Rev. B **54** (1996) 7489.
- 28) M. Fujita, H. Goka, K. Yamada, J. M. Tranquada and L. P. Regnault: Phys. Rev. B **70** (2004) 104517.